

Supplementary Figures

Fig. S1. Generation of BAP1-deficient mice.

(A) Lox sites flanked *Bap1* exons 4 and 5, the latter encoding critical catalytic residue Cys 91. Chimeric mice derived from homologous recombinant ES cells were crossed with FLP recombinase deleter mice to remove the neo selection cassette inserted between exons 3 and 4. Mice carrying the floxed *Bap1* allele (*Bap1^{fl}*) then were crossed to general Cre recombinase deleter mice to obtain the knockout (KO) *Bap1* allele. It is worth noting that *Bap1* is very close to neighboring gene *Phf7* but we did not detect altered *Phf7* gene expression in *Bap1^{-/-}* cells (data not shown). Red arrows indicate the binding sites of the

PCR primers used for *Bap1* genotyping. The agarose gel shows the wild-type (WT) and KO bands obtained when genotyping E8.5 embryos from *Bap1*^{+/-} x *Bap1*^{+/-} matings.

(B) Genotypes obtained from *Bap1*^{+/-} x *Bap1*^{+/-} matings at different developmental stages.

(C) Representative E8.5 *Bap1*^{+/+} (WT) and *Bap1*^{-/-} (KO) embryos.

(D-F) *Bap1* deletion in different *Bap1*^{fl/fl} creERT2⁺ tissues at 1 week after tamoxifen injection was assessed by PCR (D), Taqman (E), and western blotting (F). *Bap1* mRNA expression (E) is plotted relative to WT LSK cells, which are assigned a value of 100%. Splenocytes are blotted in (F). The asterisk represents a non-specific band.

Fig. S2. BAP1-deficient lymph nodes exhibit neutrophilia.

Absolute number of CD11b⁺Gr1⁺ neutrophils in the lymph nodes. Graph shows the mean ± standard deviation of at least 3 mice of each genotype.

Fig. S3. Abnormalities in BAP1 KO peripheral blood at 4 weeks after tamoxifen injection.

Fig. S4. Inflammatory infiltrates in BAP1 KO heart.

Haematoxylin and eosin staining of BAP1 KO heart revealed microthrombi (black arrow) with multifocal necrosis, neutrophilic inflammation and infiltration of myeloblastic cells not seen in WT controls. Images are representative of at least 3 mice of each genotype.

Fig. S5. Elevated LSK and myeloid progenitor cells in BAP1 KO spleen and bone

marrow.

(A) Flow cytometric analysis of spleen and bone marrow cells after gating on lineage⁻ cells. Red boxes indicate the percentage of lineage⁻ c-Kit⁺ ScaI⁻ myeloid progenitors and lineage⁻ c-Kit⁺ ScaI⁺ (LSK) cells.

(B) Gene set enrichment analysis of WT and BAP1 KO LSK cell microarray data. B lymphocyte progenitor and intrathymic T progenitor gene sets are down-regulated, whereas a subset of myeloid enriched genes are up-regulated in BAP1 KO cells.

(C) A subset of genes whose expression is dysregulated in BAP1 KO LSK cells.

Fig. S6. Colony formation assays with BAP1 KO LSK cells.

(A, B) FACS-sorted LSK cells were plated in methylcellulose media supplemented with cytokines (Methocult media M3434, unlike M3534, contains erythropoietin and therefore supports growth of a broader range of progenitors). Asterisks indicate statistically significant differences between WT and KO cells based on two-way ANOVA analysis. *** P<0.001. Graphs show the mean ± standard deviation of at least 3 mice of each genotype.

(C-D) Cytospins and Wright-Giemsa staining of cells at 10 days after the initial plating (C) and at 10 days after replating equal numbers of cells in C (D). Representative images are shown of cells grown in methocult M3534 media. Cultures were prepared for 3 mice of each genotype.

Fig. S7. BAP1 KO lineage-depleted progenitors show impaired reconstitution potential.

Lineage-depleted progenitors were isolated from CD45.2⁺ WT and BAP1 KO bone marrow at 1 week (**A**) or 1 month (**B**) after the final tamoxifen injection. The cells were transplanted into lethally irradiated CD45.1⁺ recipients. The percentage of CD45.2⁺ peripheral blood leukocytes in reconstituted recipient mice was determined by flow cytometry at the times indicated. All graph show the mean \pm standard deviation of at least 3 mice of each genotype. Asterisks indicate statistically significant differences between WT and KO mice based on two-way ANOVA analysis, followed by Bonferroni post-test analysis. * P<0.05, *** P<0.001, **** P<0.0001.

Fig. S8. BAP1 KO bone marrow shows impaired reconstitution potential in competitive transplantation assays.

CD45.1⁺ WT bone marrow cells were mixed in a 1:1 ratio with either CD45.2⁺ WT (black bars) or BAP1 KO (red bars) bone marrow cells harvested 1 week after the final tamoxifen injection. The cell mixtures were transplanted into lethally irradiated CD45.1⁺ recipients, and the ratio of CD45.1⁺ cells to CD45.2⁺ cells in peripheral blood was determined by flow cytometry at the times indicated. All graph show the mean \pm standard deviation of at least 3 mice of each genotype. Asterisks indicate statistically significant differences based on two-way ANOVA analysis, followed by Bonferroni post-test analysis. * P<0.05, *** P<0.001, **** P<0.0001.

Fig. S9. Reconstitution of lethally-irradiated CD45.1⁺ WT recipient mice with CD45.2⁺ *Bap1*^{+/+} creERT2⁺ or *Bap1*^{fl/fl} creERT2⁺ bone marrow cells. Peripheral blood was analyzed by flow cytometry at 5 weeks after reconstitution. Histograms indicate the

percentage of leukocytes staining positive for CD45.2. Histograms are representative of 3 mice of each genotype.

Fig. S10. Generation of BAP1.3xFlag and 3xFlag.ARMIC8 knock-in mice.

(A) BAP1.3xFlag mice contained the 3xFlag sequence just ahead of the *Bap1* translation termination codon within exon 17. A neo selection cassette inserted between exons 16 and 17 was deleted from homologous recombinant ES cells with FLPe recombinase adenovirus.

(B) Western blotting of wild-type (WT) and BAP1.3xFlag spleen and brain.

(C) 3xFlag.ARMIC8 mice contained the 3xFlag sequence just after the *Armc8* translation initiation codon within exon 1. A neo selection cassette inserted within a less conserved *Armc8* promoter region was removed by crossing the chimeras to FLP recombinase deleter mice.

(D) Silver staining of anti-Flag immunoprecipitations from WT, BAP1.3xFlag, and 3xFlag.ARMIC8 spleens.

Fig. S11. BAP1 expression in hematopoietic cell types..

Western blotting of WT and BAP1.3xFlag cells.

Pooled cells from 3-5 mice of each genotype were analyzed.

Fig. S12. Characterization of OGT as a substrate of BAP1.

(A) Ubiquitin (ub)-AMC assay. Red line shows inactivation of BAP1 upon pre-treatment with 20 mM N-ethylmaleimide (NEM) for 15 minutes at room temperature.

(B) Western blotting of WT and BAP1 KO mouse embryonic fibroblasts treated with 10 µg/mL cycloheximide (CHX) for the times indicated.

Fig. S13. HCF-1 and OGT binding sites in WT BMDMs identified by ChIP-sequencing.

Fig. S14. An inactivating *BAP1* mutation identified in a *de novo* MDS patient sample. Sanger sequencing of tumor cells identified *BAP1* mutation p.Ala82fs, which results in premature termination and is within the UCH enzymatic domain. This mutation was not detected in normal cells from the same patient. Forward (F) and reverse (R) strand reads are shown.

Fig. S15. BAP1 expression is reduced in MDS patients.

Box and whisker plot of *BAP1* gene expression in bone marrow cells from MDS patients and control individuals (normal) based on microarray dataset GSE30195. *BAP1* expression is significantly lower in MDS patients (p-value=0.0035, Student's t-test).

Fig. S16. Mild, progressive hematological defects in BAP1 heterozygous mutant mice.

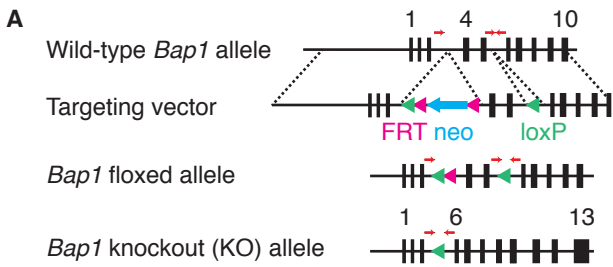
(A) *Bap1* deletion in spleen after tamoxifen injection was assessed by PCR.

(B-F) Peripheral blood cell counts. All graphs show the mean ± standard deviation for 3 mice of each genotype. Asterisks indicate statistically significant differences between WT and BAP1 KO mice based on one-way ANOVA analysis followed by Bonferroni post-test analysis. * P<0.05, *** P<0.001, **** P<0.0001.

Fig. S17. Expression of *hox* genes in BAP1 KO cells.

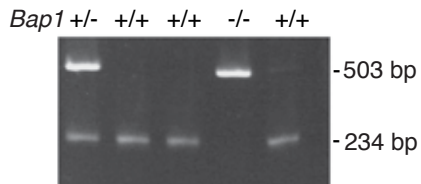
Microarray data analyses of FACS sorted lineage⁻ ScaI⁻ c-Kit⁺ myeloid progenitors (MP), lineage⁻ ScaI⁺ c-Kit⁺ (LSK) cells, lineage⁻ bone marrow progenitors, and CD11b⁺ myeloid cells.

Fig. S1



B

Developmental stage	<i>Bap1</i> +/+	<i>Bap1</i> +/-	<i>Bap1</i> -/-	Total no.
E8.5	6	18	9	33
E9.5	14	7	3	24
E11.5	21	7	0	28
PO	23	28	0	51



C



hf=head folds; nt=neural tube; a=allantois

D

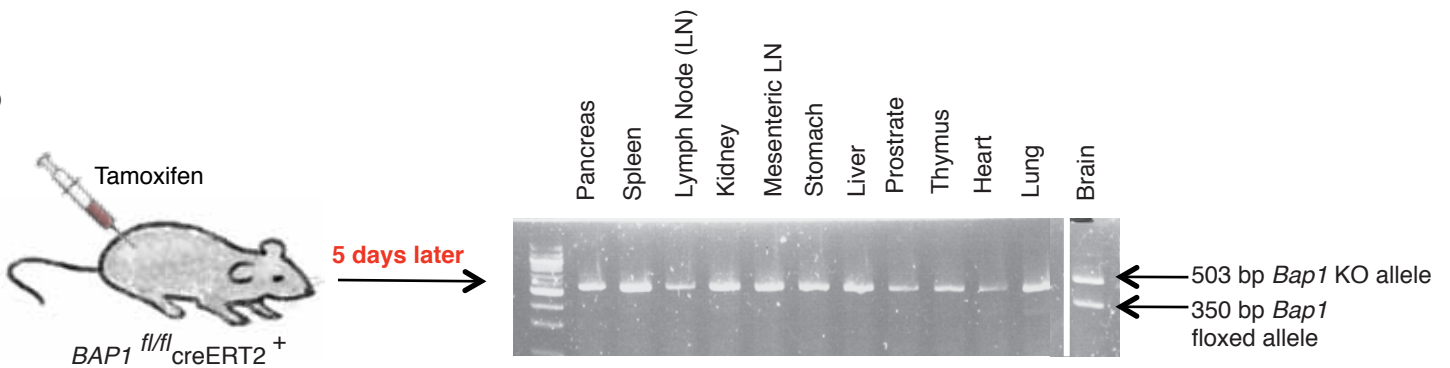
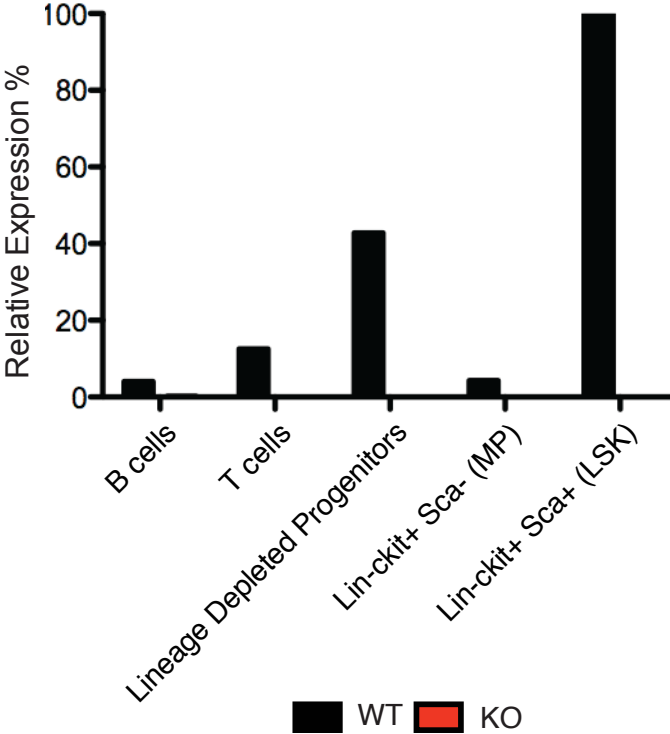


Fig. S1

E



F

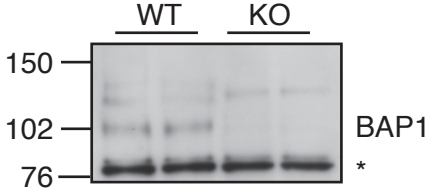


Fig. S2

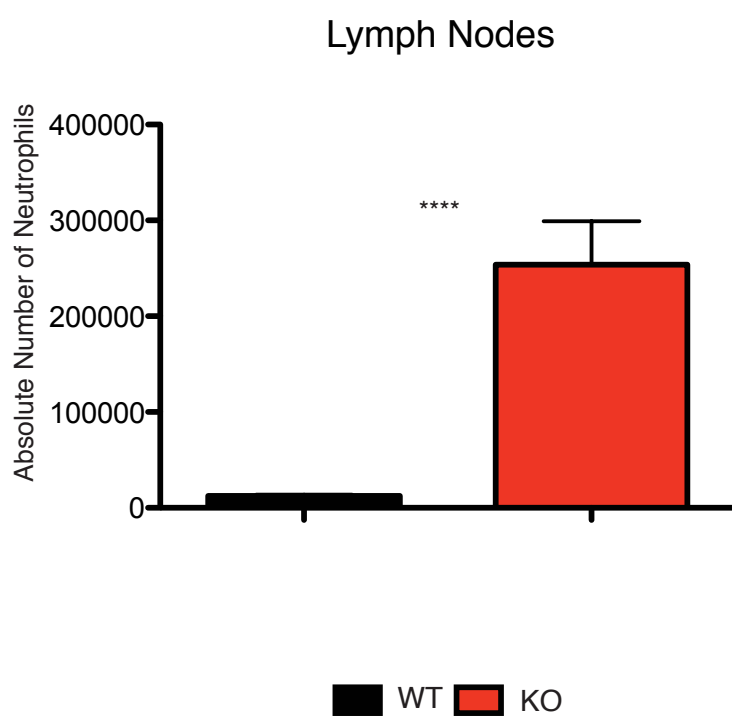
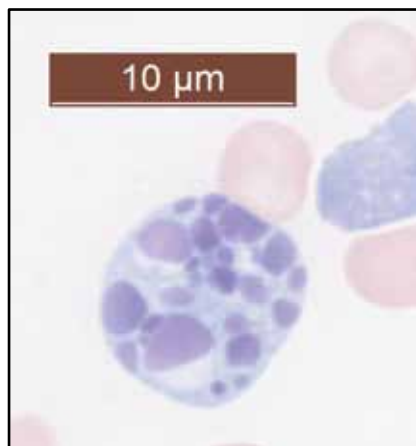


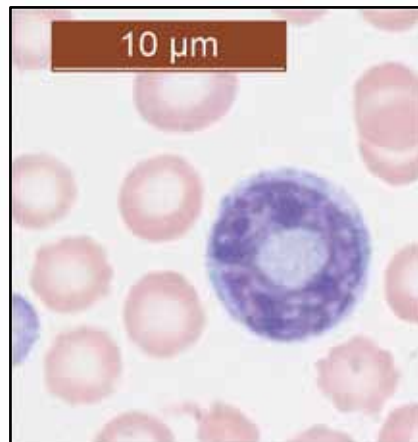
Fig. S3

KO

Apoptotic Cell



Ringed Nuclei



Mitotic Cell and Post-Mitotic Nuclei

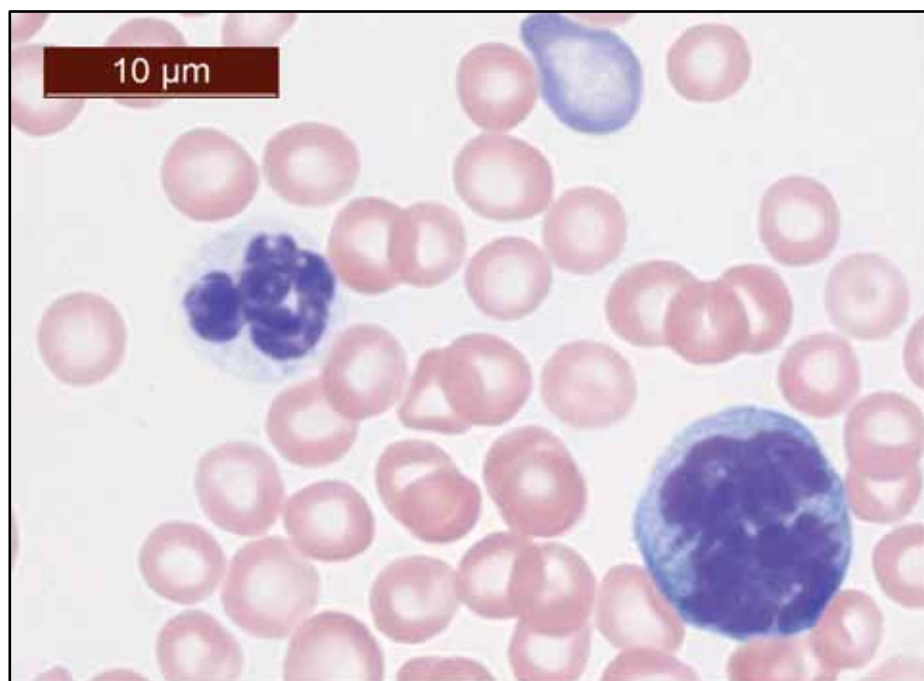
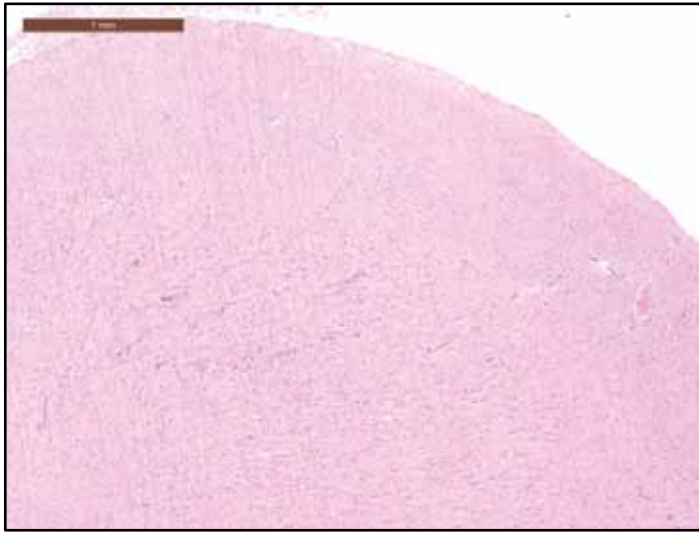
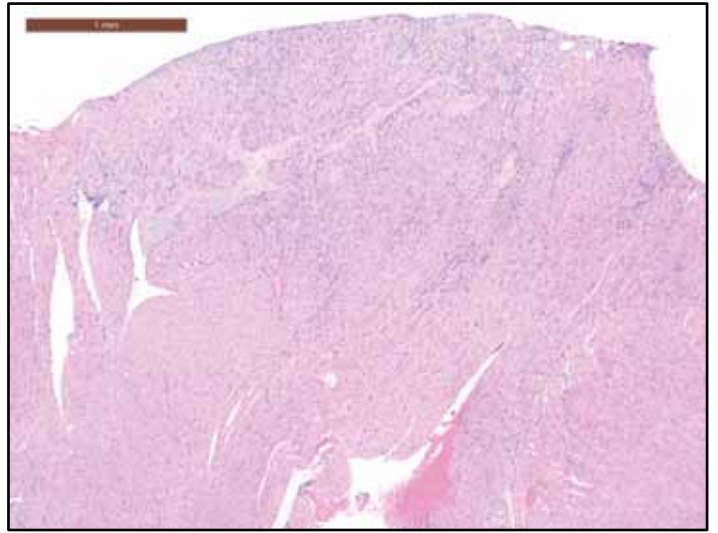


Fig. S4

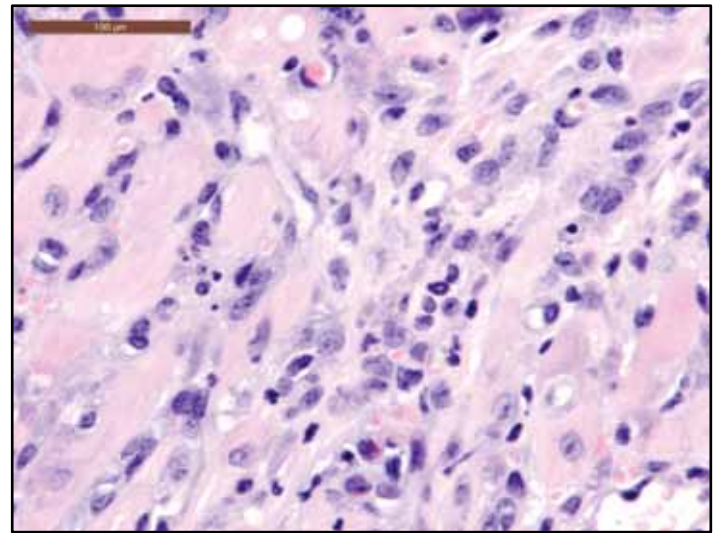
WT



KO



KO



WT

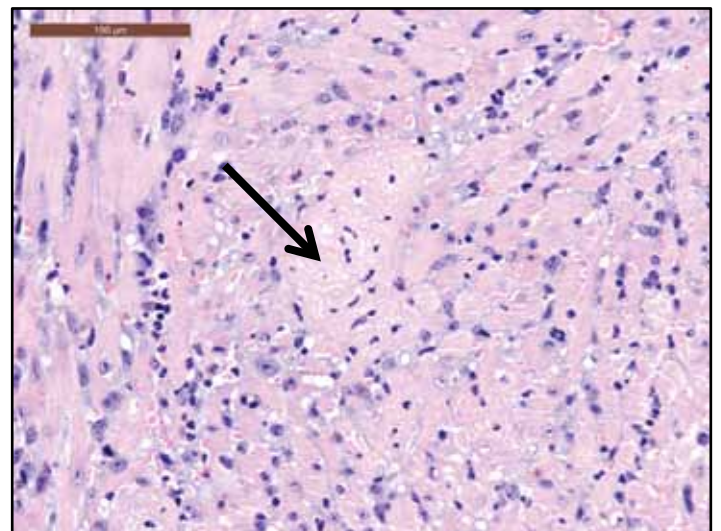
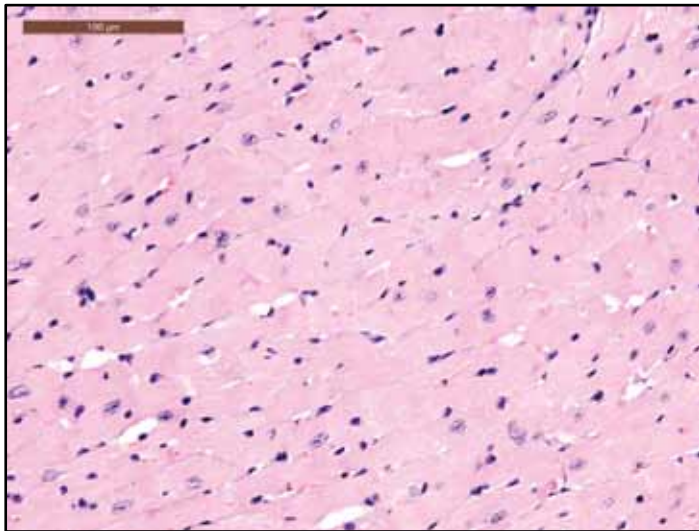


Fig. S5

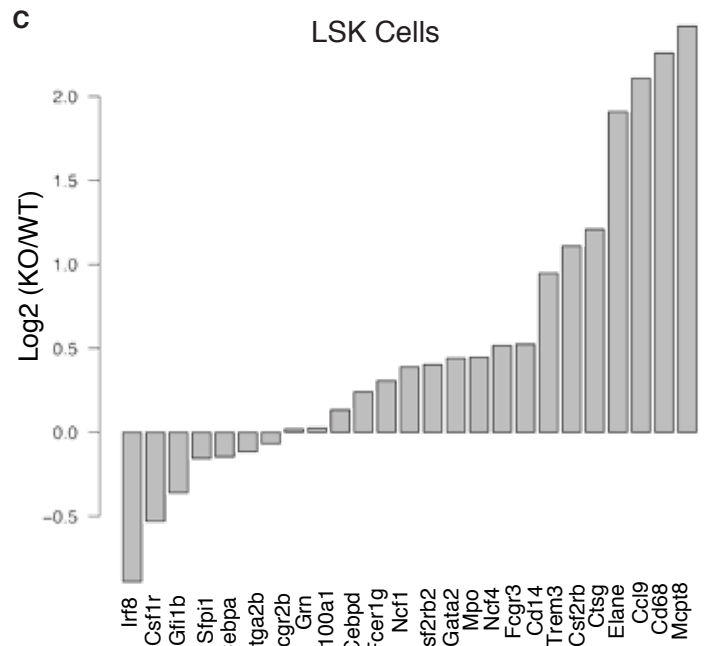
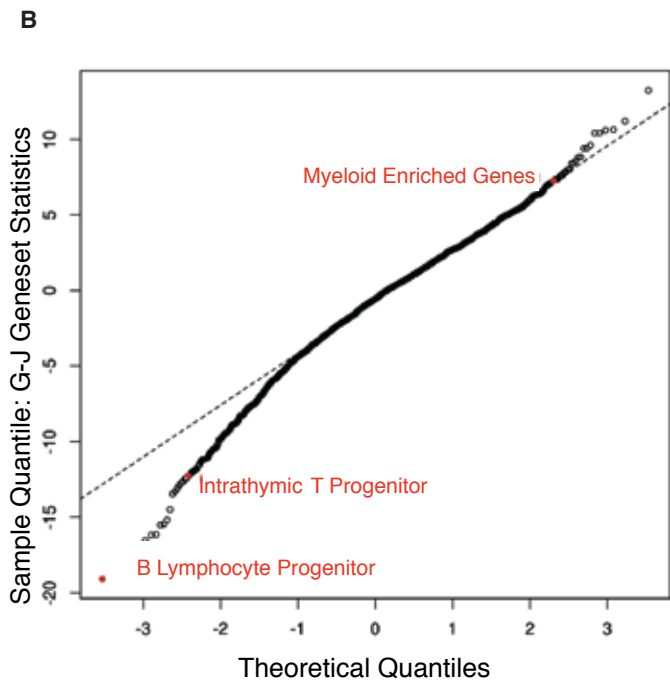
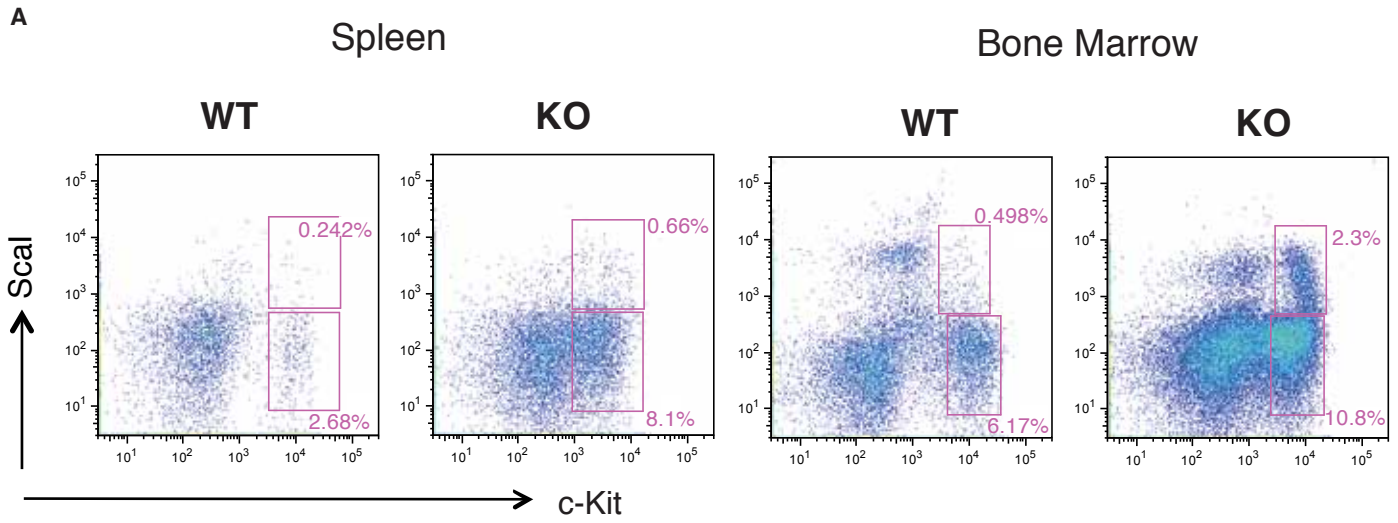


Fig. S6

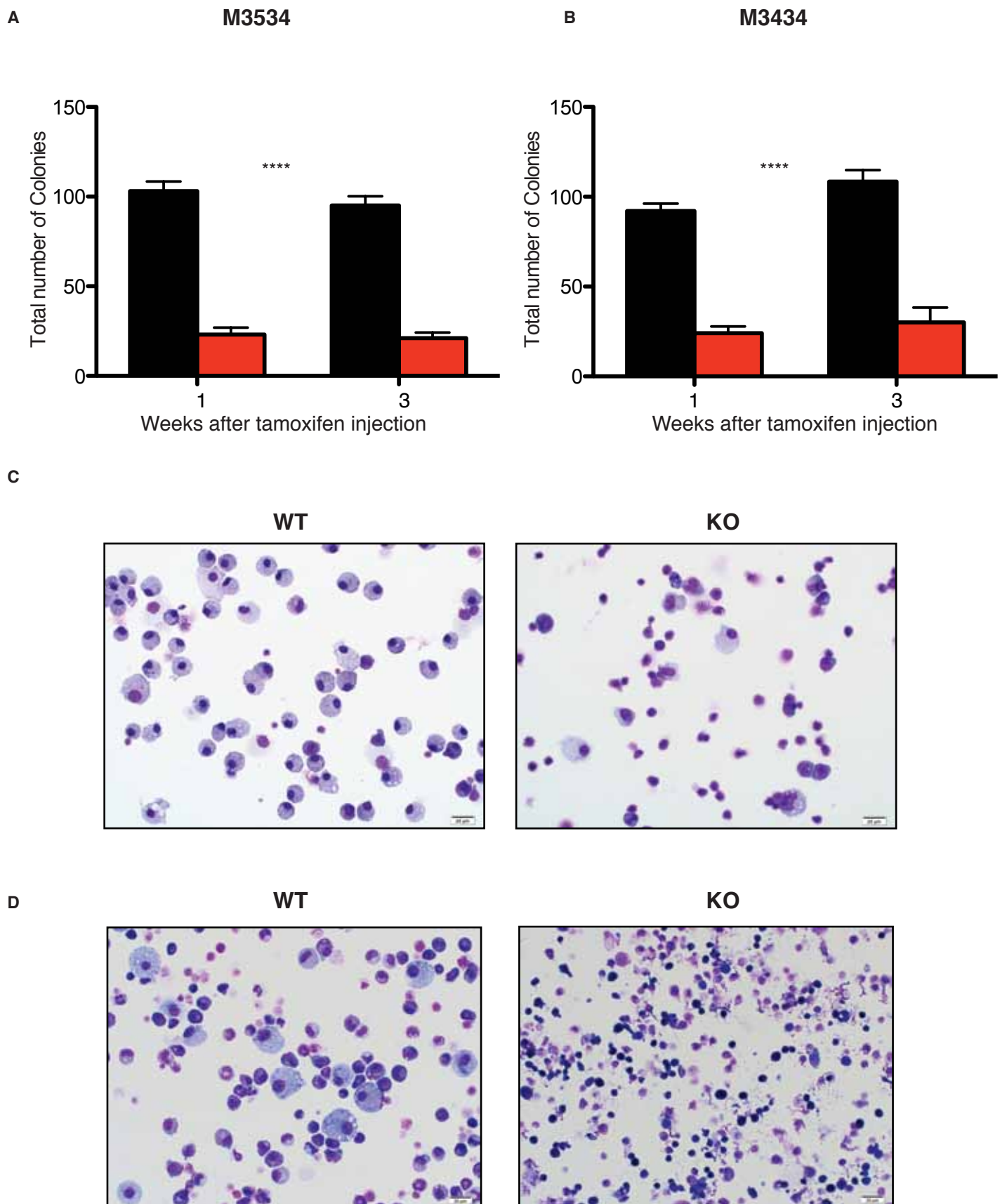


Fig. S7

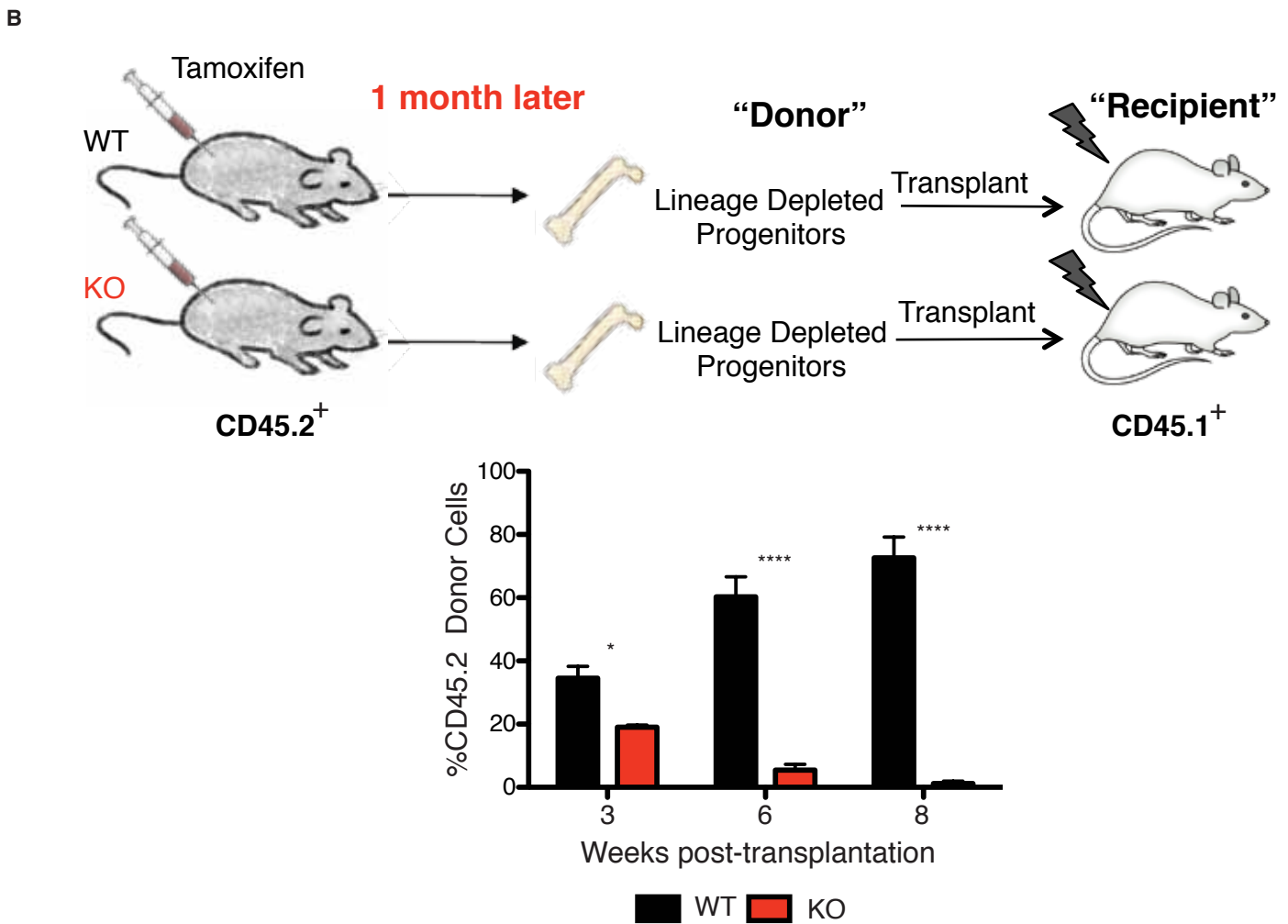
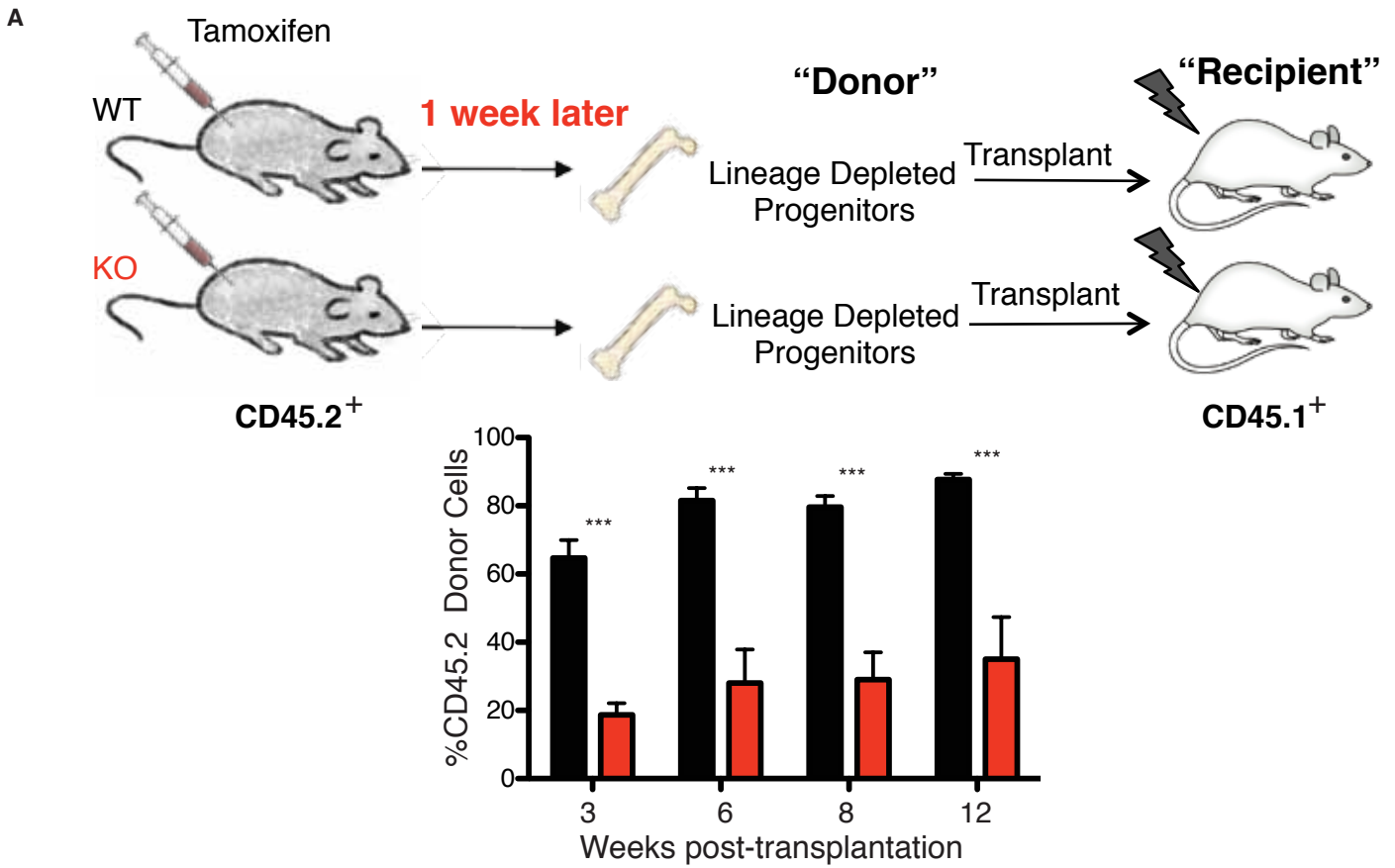


Fig. S8

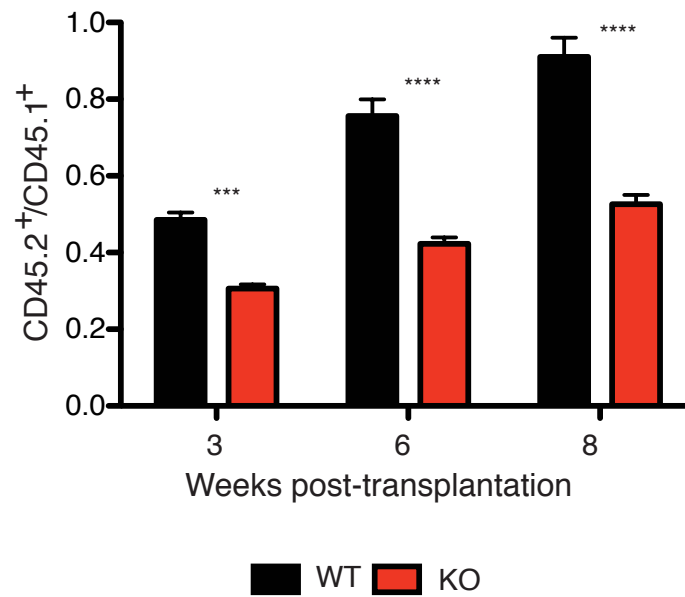
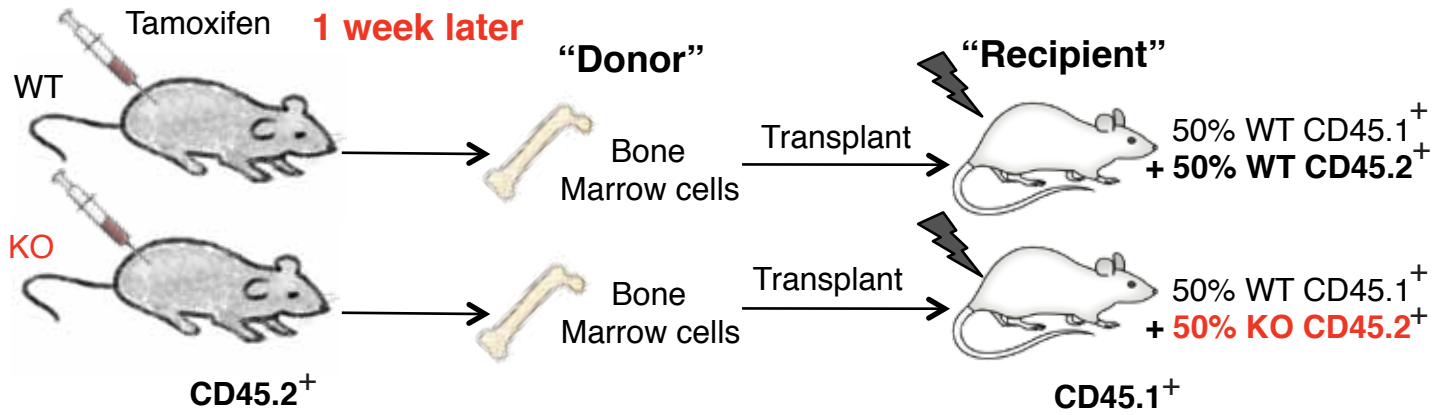


Fig. S9

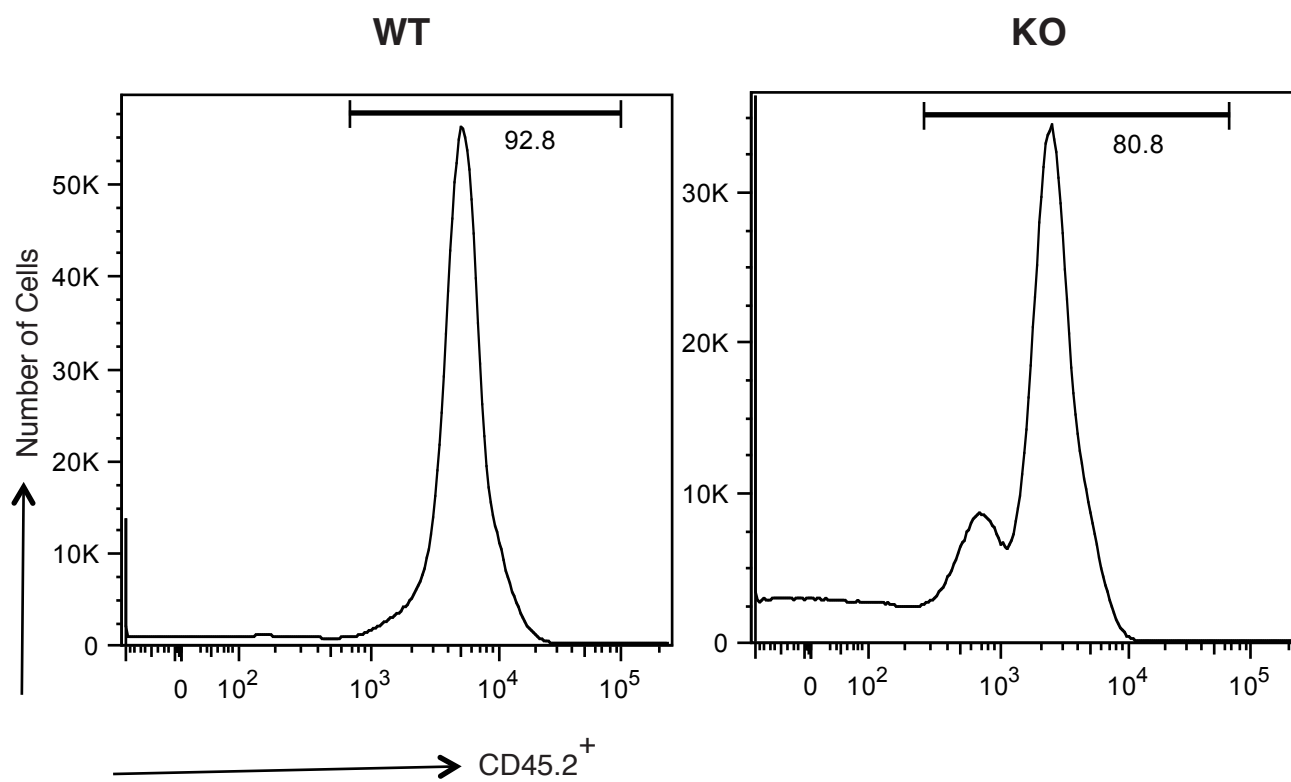


Fig. S10

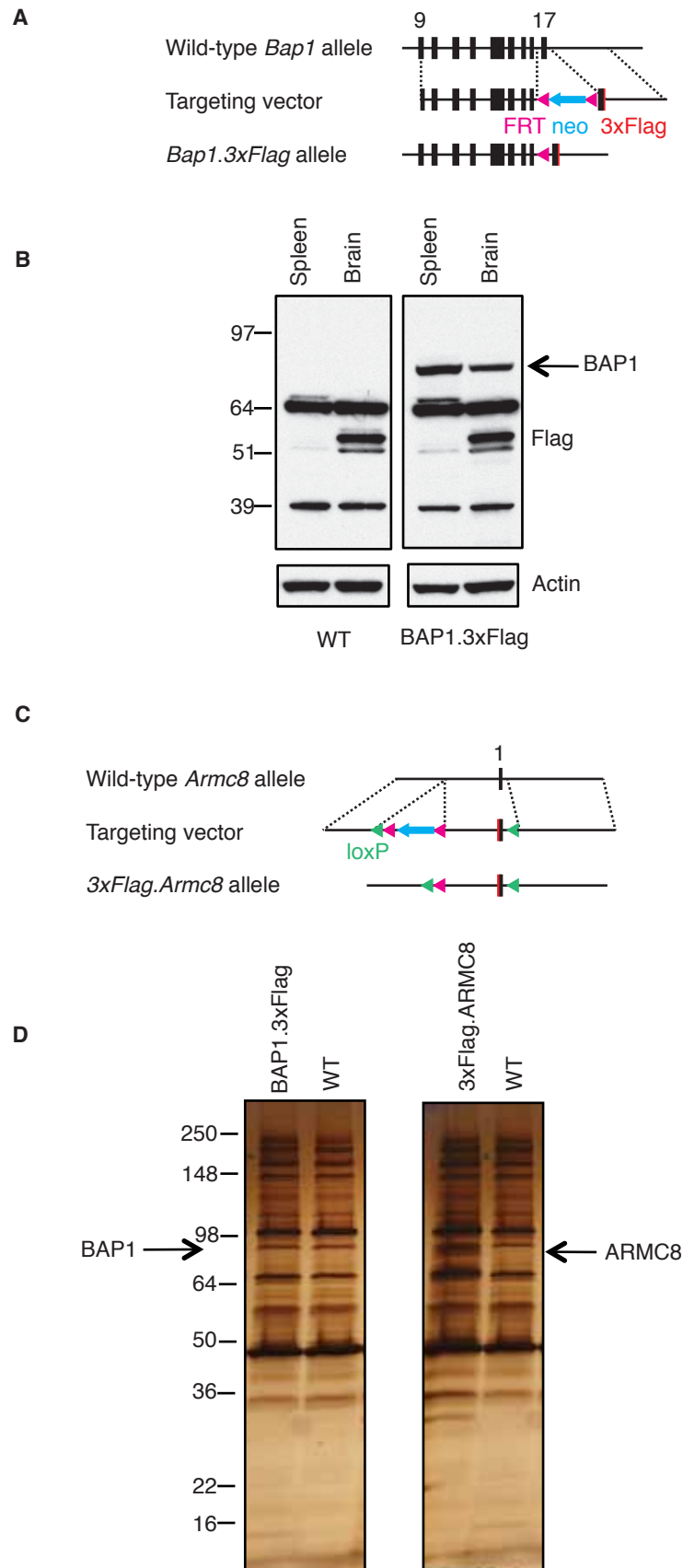


Fig. S11

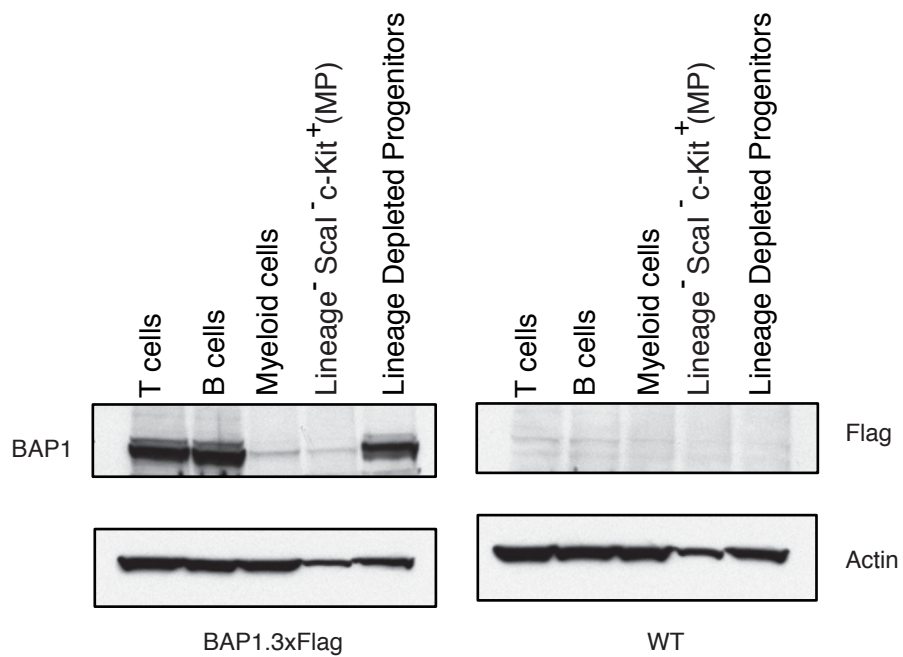
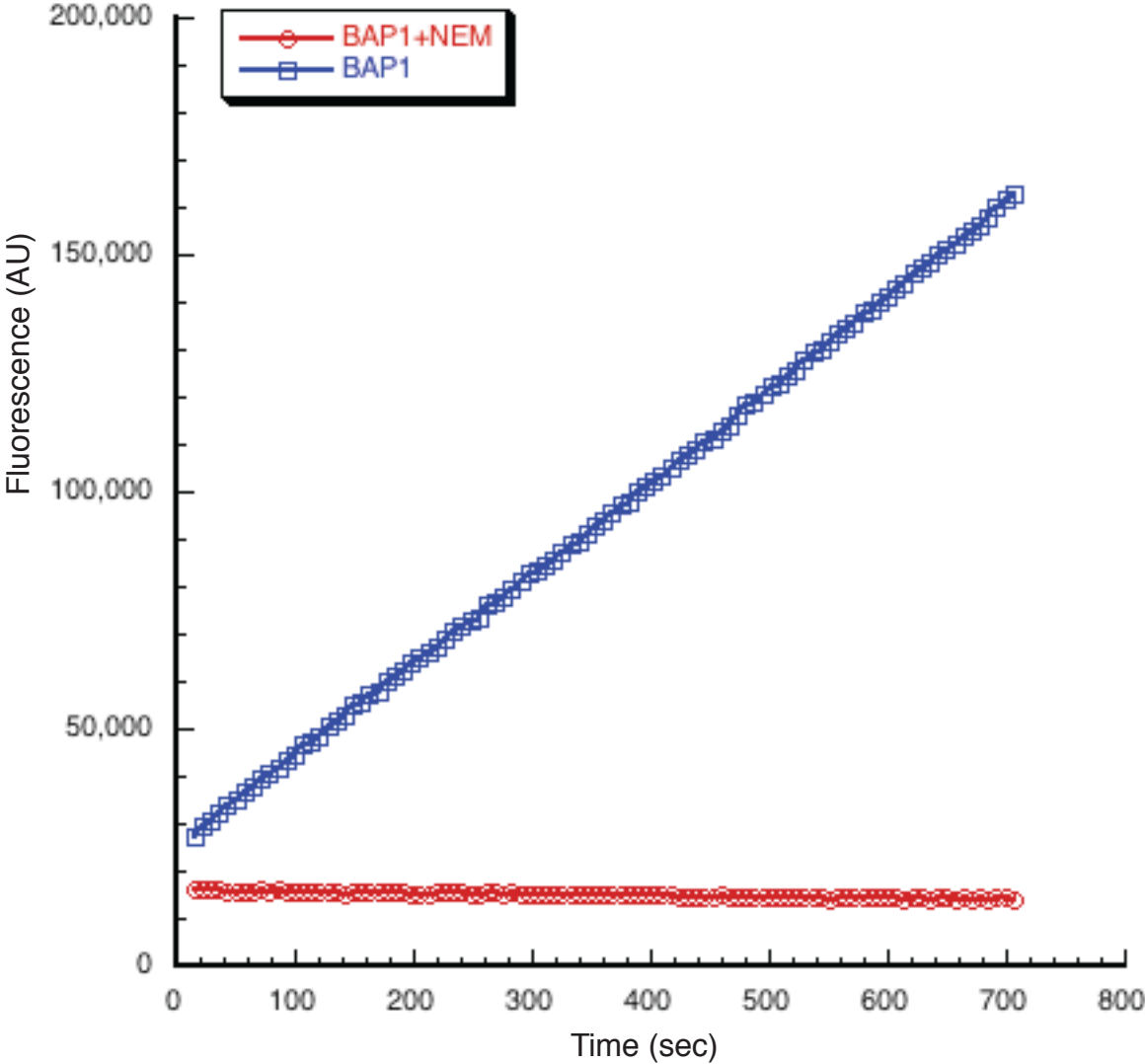


Fig. S12

A



B

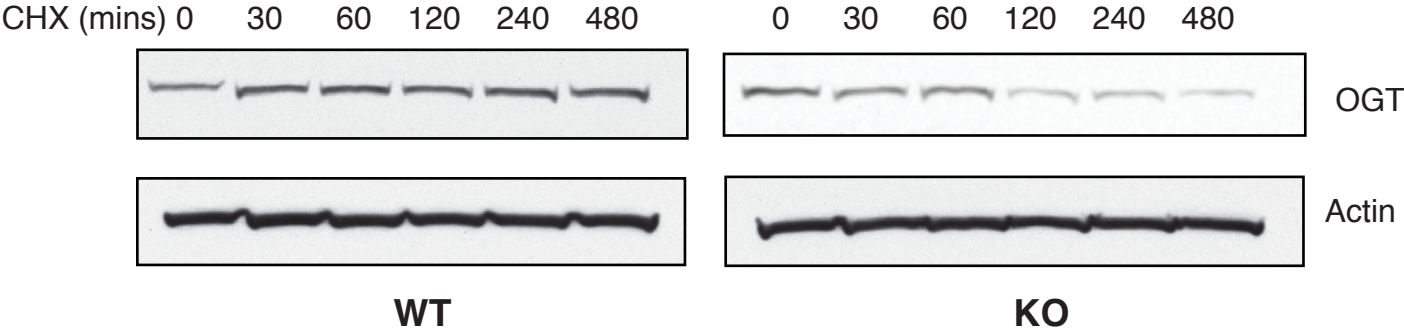
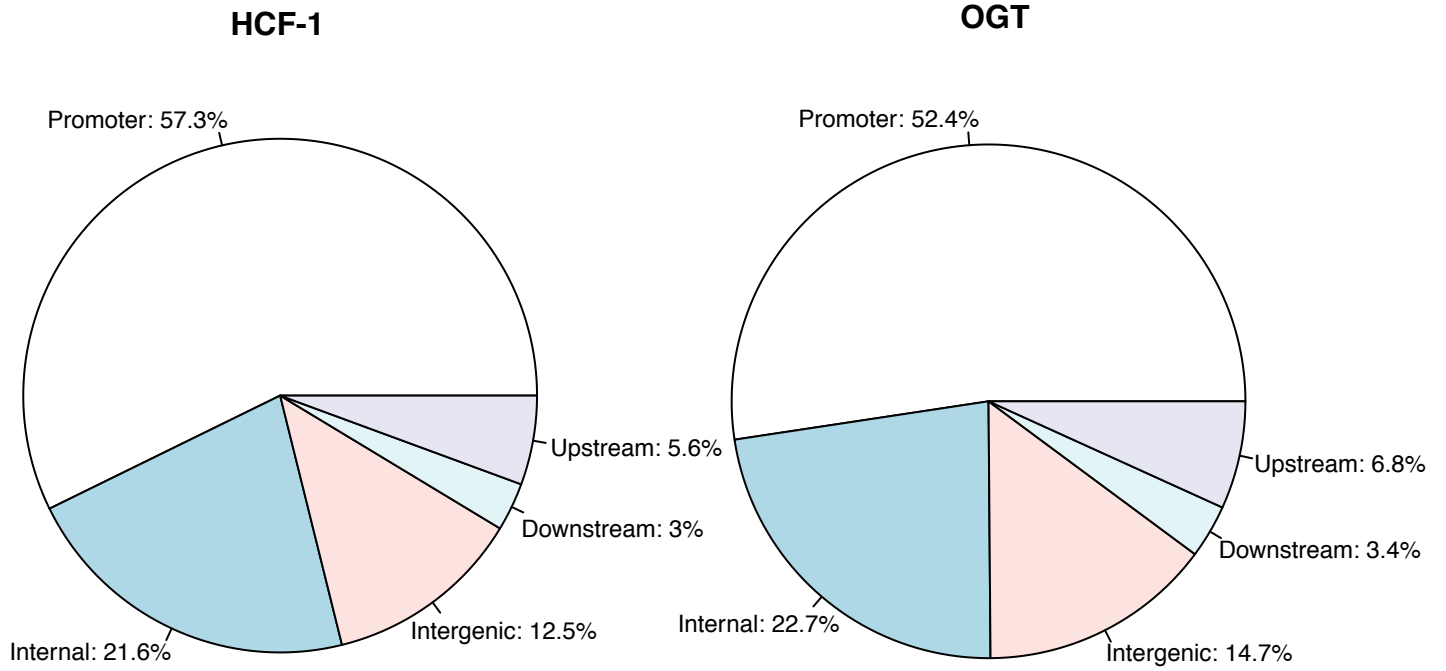
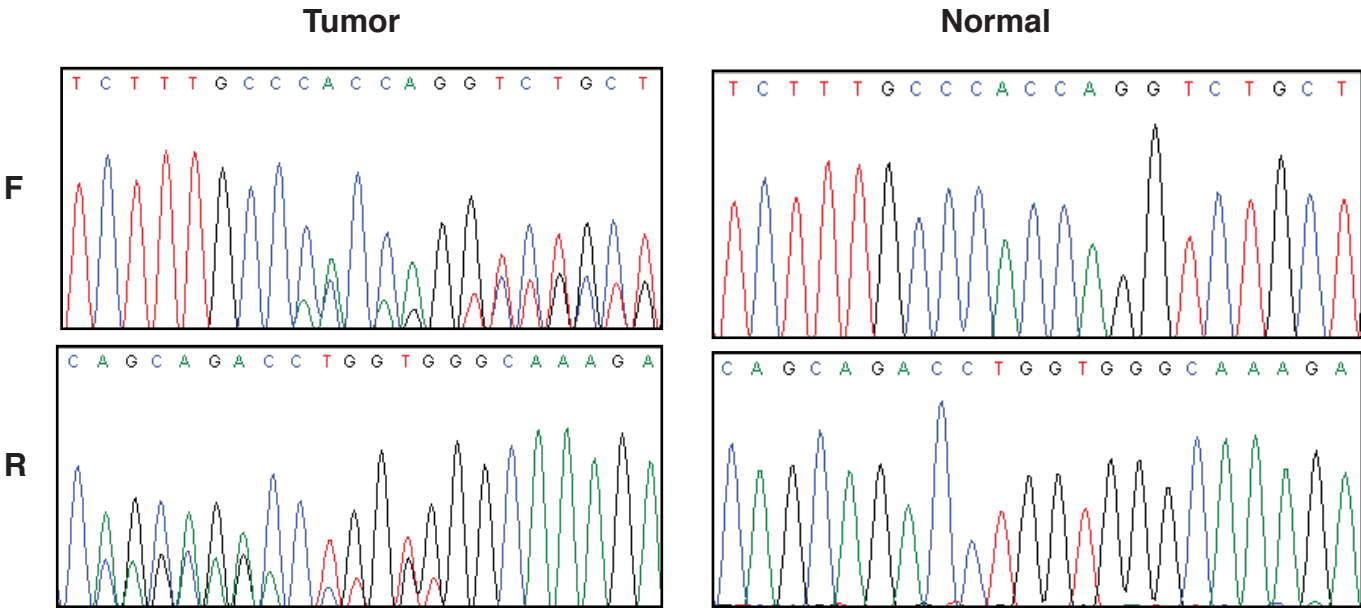


Fig. S13



Promoter: +/- 2kb of TSS
Downstream: 8kb from gene end
Upstream: -2kb to -8kb from TSS

Fig. S14



c.248delC
p.Ala82fs
Results in STOP 3 amino acids later at amino acid 85

Fig. S15

BAP1 (201419_at): GSE30195

p_val= 0.00351

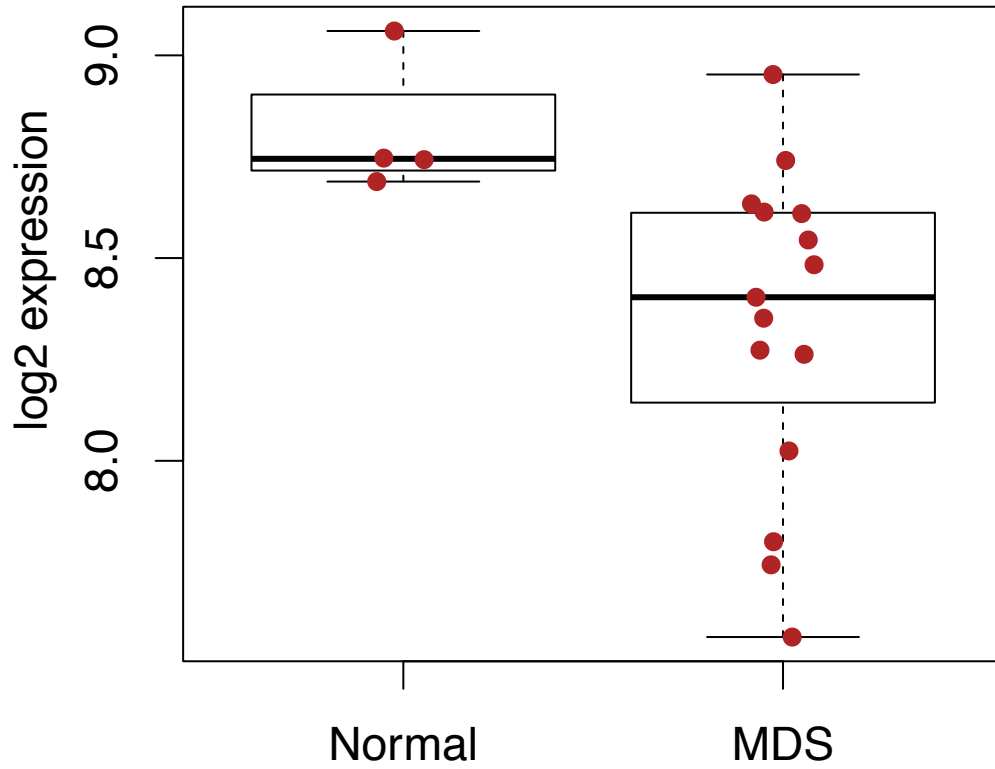


Fig. S16

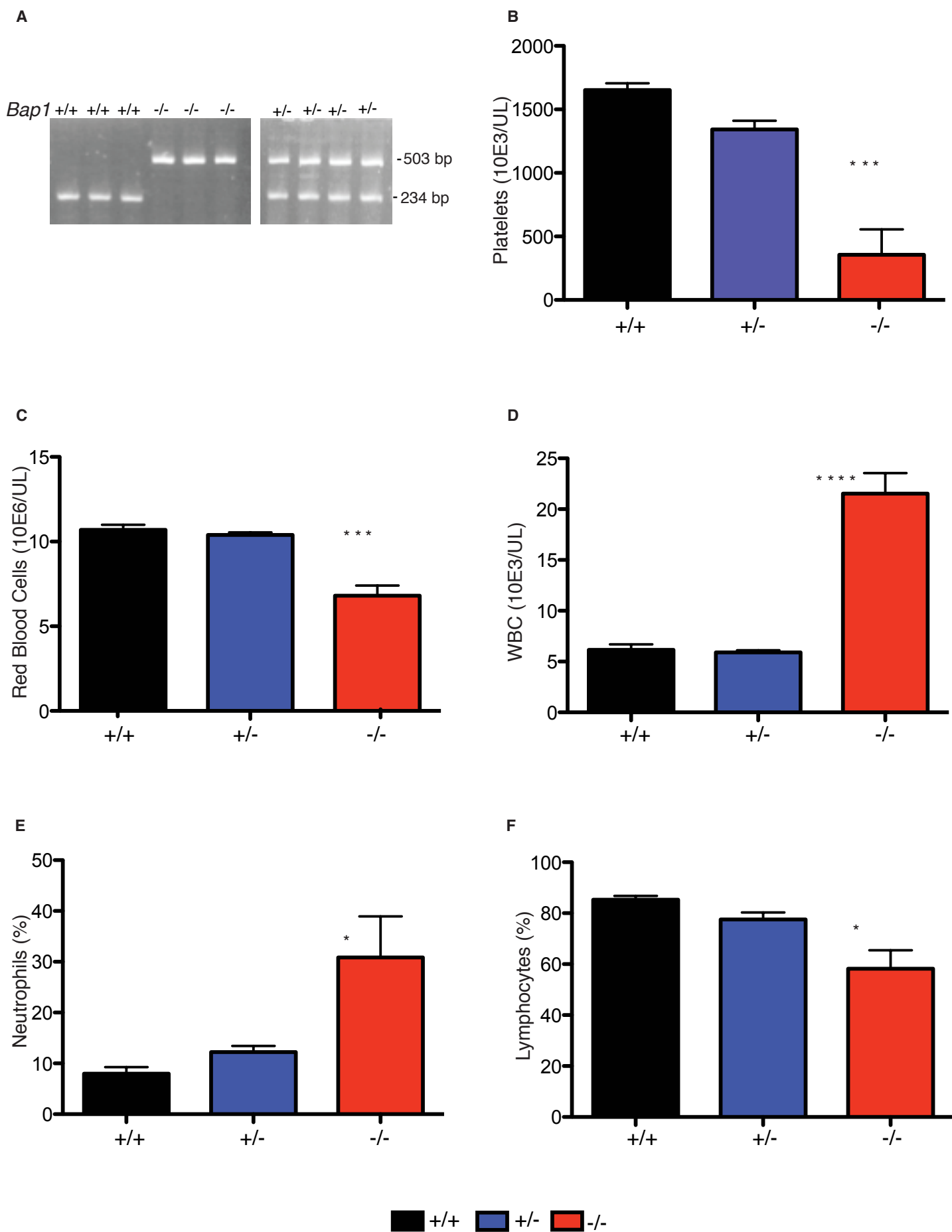


Fig. S17

